DOE/ER/01388-480

Coincidence Study of the $^{27}Al(^{16}O, {}^{12}C\alpha)^{27}Al$ Reaction at 65 MeV*

M.B. Tsang, W.G. Lynch, R.J. Puigh, R. Vandenbosch and A.G. Seamster

Nuclear Physics Laboratory

University of Washington

Seattle, Washington 98195

Abstract: Both in-plane and out-of-plane angular correlations of coincident C and α particles have been measured for 65 MeV ^{16}O bombardment of an ^{27}Al target. Exploitation of the time-of-flight method enabled measurement of very low energy alpha particles at back angles. Results from the present experiment show that evaporation from an intermediate nucleus $^{31}P^*$ accounts for the majority of the C-α coincidence events observed. A small number of alpha particles from the break-up of $^{16}O^*$ were detected at angles around that of the carbon detector. Less than 10% of the alpha particles detected are of pre-equilibrium origin. This is in sharp contrast to earlier results.

[NUCLEAR REACTION $^{16}O + {}^{27}Al$. E_{lab} = 65 MeV

measured $d^2\sigma/d\Omega_c d\Omega_\alpha$, C-α coin, ^{27}Al tgt]

DISCLAIMER

Blank Page

I. Introduction

In the past several years, there has been an increased interest in prompt or pre-equilibrium light particle emission in heavy ion reactions[1-10]. Light particle emission often accompanies peripheral collisions in which a projectile-like and target-like product are also produced. These light particles can either be produced during the collision itself or can arise from sequential decay of the target-like or projectile-like products. The sequential decays can possibly be pre-equilibrium if the decay occurs prior to complete equilibration of the dissipated energy, or evaporative if equilibrium has been attained. For not too heavy reaction products alpha evaporation can be an important decay process of the equilibrated products since in deeply inelastic collisions, a considerable amount of angular momentum can be transferred from the relative motion of the target and projectile into the internal degrees of freedom of the reaction products. Alpha particle emission is an important evaporative decay process since it can carry away large amounts of angular momentum. For mass-asymmetric binary reactions one can ask whether the bulk of the sequential alpha particles originate from the projectile-like or target-like fragment. The current experimental evidence indicates only that both fragments can emit alpha particles and no systematic behavior has been established as yet.

Many models have been proposed to describe the mechanisms for producing pre-equilibrium alpha particles[11-14]. Two simple

and illustrative models are the "piston model" and the "hot spot" model. The "piston model" was first discussed by Gross and Wilczynski[11]. In this model, the alpha particles induced by the radial component of the dissipative force are emitted in the early stage of collision. The alpha particles are "shot" through the nucleus perhaps knocking out other alpha particles and emerge on the other side of the nucleus from the point of impact. The "hot spot" model was first proposed by Gottschalk and Westrom[12] in connection with the reaction $^{58}Ni(^{16}O,\alpha x)$ at 92 MeV investigated by Ho et al[6]. In this model, the incident particle excites ("heats up") a localized part of the target nucleus and that localized region subsequently de-excites by alpha emission.

None of the available models explain all the pre-equilibrium alpha particle data. This lack of a global understanding of the heavy ion-alpha angular correlation data may arise from the fact that contributions of alpha particles from other processes such as evaporation and projectile break up have not been fully taken into account. In order to extract the different components of the alpha emission, it is necessary to take angular correlation data over a wide angular range including both in-plane and out-of-plane angles. The work described here consists of such a comprehensive study conducted to understand the nature of alpha particle emission in the light heavy ion system $^{27}Al + ^{16}O$ at 65 MeV.

The earlier work of Harris et al. on the system $^{27}Al + ^{16}O$ at 65 MeV suggested that sequential pre-equilibrium alpha emission

from $^{31}P^*$ (E_x=14.5 MeV) is the dominant mechanism for producing alpha particles in coincidence with carbon particles[1]. Such a mechanism can be represented as follows:

$$^{27}Al + ^{16}O \rightarrow ^{12}C + ^{31}P^*$$

$$^{31}P^* \rightarrow \alpha + ^{27}Al$$

The carbon singles energy spectra obtained were approximately gaussian in shape with a peak at about 44 MeV for θ_c=-30°. If two-body kinematics is assumed, $^{31}P^*$ has a most probable excitation energy of about 14.5 MeV. The angular correlation data of Harris et al., indicated by "*", are plotted in the center of mass system of $^{31}P^*$ in Fig. 1. Very few alpha particles were observed past 90° in the center of mass system indicating the absence of an evaporative component. The result obtained was interesting since it implied that the mechanisms for producing pre-equilibrium alphas could be studied with a relatively simple system at low energies. The present work was originally designed to explore the region at backward angles by improving the ability to detect low energy alphas and to better determine the contribution of the evaporation component from $^{31}P^*$ by taking out-of-plane angular distribution data in addition to the in-plane backward angle data.

II. Experimental Method

The experiment was performed by bombarding ^{27}Al with 65 MeV ^{16}O ions from the University of Washington FN tandem Van de Graaff. Carbon and alpha particles were detected in coincidence.

Fig. 2 shows a schematic view of the experimental set-up. The reaction plane is defined by the beam and the carbon telescope. Angles on the same side as the carbon telescope are defined to be negative. Out-of-plane angles are in the plane containing the recoil direction of $^{31}P^*$. Both in-plane and out-of-plane C-α angular correlations have been taken at $\theta_c=-30^\circ$. Since the scattering chamber is not equipped with an out-of-plane movable arm, data were taken at 30° intervals for the out-of-plane angular correlation.

The carbon detector consisted of a DE-E Si telescope counter. During the course of the experiment, three different DE counters (14.7 μ, 17.3 μ, and 20 μ) were used. The carbon detector typically subtended a solid angle of ~ 8 msr, and was fixed at 30° for all of the measurements reported here.

Two methods have been used to identify the alpha particles: (1) DE-E counter telescope method, and (2) the time-of-flight method.

The DE-E counter telescope method is the most common technique used in particle-particle coincidence experiments[1-10]. In order to increase the efficiency of detecting low energy alpha particles at backward angles, two different DE-E telescope systems were used to detect alpha particles. For the backward angles past 90° and -60°, a 5μ-300μ DE-E telescope counter subtending a solid angle of ~ 5 msr was used. For more forward angles, a 8.7μ-300μ thick DE-E telescope subtending a solid angle of 1.5 msr was used. The alpha telescope was moved in the reaction plane defined by the

beam and the carbon detector. One disadvantage of the telescope method was cut-off of low energy alpha particles introduced by the presence of the DE detector. This drawback can be eliminated by detecting the alpha particle with a single counter using the time-of-flight method.

In the time-of-flight method, a 300μ single Si detector was placed at ~ 20 cm from the target. The alpha particles were identified by measuring the time difference between the arrival of an event in the carbon telescope counter and the arrival of a coincident event in the single alpha counter. The carbon particles of interest typically have energies between 30 and 60 MeV. As the carbon telescope was placed ~ 7.6 cm from the target during the experiment, it took from 3.4 to 2.4 ns for the carbon particles to reach the carbon telescope counter respectively. This uncertainty of 1 ns is negligible when compared to the 5 ns timing resolution required to separate the alpha particles of interest from other particles.

This method worked well in the present system and allowed up to four single alpha detectors located at four different angles to be used in coincidence with one carbon telescope. Kinematically, the alpha particles detected at backward angles are lower in energy than those detected at the forward angles. Thus the time-of-flight method allowed the extension of the C-α angular correlation function to more backward angles.

Both the carbon and alpha detectors were calibrated with the corresponding particles. The carbon telescope was calibrated

with 30, 44 and 60 MeV carbon beams from our sputter source while the alpha detectors were calibrated with 5.5 MeV α's from a ^{241}Am source and 8.78 MeV α's from a ^{212}Po source. All the detectors were thermo-electrically cooled to $0^{o}C$ to suppress noise and leakage current of the counters. Area-defining circular tantalum apertures, mounted directly in front of the detectors, were covered with 98 $\mu g/cm^2$ Ni foils to avoid condensation of pump oil onto the detector surface.

The self-supporting ~1mg/cm^2 ^{27}Al targets were produced by vacuum evaporation of 99.999% pure ^{27}Al wire. The oxygen and carbon contents in these targets were determined by backward angle scattering of 3 MeV protons[13,14]. These elements (carbon and oxygen) were shown to be present originally in less than 1% atomic abundance. Back-streaming of mechanical pump oil into the scattering chamber during the experiment caused a layer of carbon to be formed on the part of the target hit by the beam. The $C(^{16}O,C\alpha)$ events are kinematically separated from the $^{27}Al(^{16}O,C\alpha)$ events with Q=-7.16 MeV at the angles measured in this experiment. The effect of carbon build-up was studied by bombarding a 370$\mu g/cm^2$ carbon target. The total energy spectrum for events from both the $^{nat}C(^{16}O,C\alpha)$ and $^{27}Al(^{16}O,C\alpha)$ reactions at $\theta_c=-30^{o}$ are shown in Fig. 3. While only an upper limit of carbon buildup could be measured by determining the amount of carbon in the target at the end of the experiment, nevertheless it was determined that in the region of the peak corresponding to the $^{27}Al(^{16}O,C\alpha)$ reaction leaving ^{12}C in its ground state, the

contribution from carbon build up contamination was negligible.

III. Data Analysis

Two types of events were collected during the experiment, coincidence events detected both by the carbon telescope and one of the alpha detectors and the singles events detected only by the carbon telescope. Since there were many more carbon singles events than coincidence events, the carbon singles events were prescaled by a factor of 100 before the signals were sent to the computer. All the data collected were stored event by event on a magnetic tape for later off-line analysis.

A three-body final state of $^{27}Al + ^{16}O \rightarrow ^{12}C + \alpha + ^{27}Al + Q$ was assumed in the data analysis. For most of the angles measured, two major groups of events with Q=-7.16 and Q=-11.59 MeV were observed. These two groups of events can be seen clearly in Fig. 3. The former group with Q=-7.16 MeV corresponds to events with all three final products ^{12}C, α and ^{27}Al in their ground states. The latter group of events, Q=-11.59 MeV can be either events with ^{12}C in its first excited state (2^+) or ^{27}Al in one of its excited states. The valley between these peaks is probably filled with events that correspond to residual excited states of ^{27}Al and the contributions from $^{12}C(^{16}O,C\alpha)$ and $^{16}O(^{16}O,C\alpha)$ events.

The data were analysed off line with a window placed around the Q=-7.16 MeV group of events in a E_c vs. E_α two dimensional plot. For all the data presented here except those shown in

Fig. 3, contributions due to accidental coincidence were subtracted. In general, the random events were only a small fraction of the total events, less than 5% for the forward angles. However, the percentage of the random events was as high as 15% at backward angles and at angles on the same side as the carbon telescope.

Since the carbon detector was fixed throughout the experiment, the carbon singles events detected by the carbon detector during each experimental run were used to normalize data from different runs.

IV. Experimental Results

One way of presenting all the data taken in a particular plane at a glance is to plot the data in the Gallilean invariant velocity space[17] i.e. the quantity $d^4\sigma/d\Omega_c^{lab}d^3v_\alpha^x$ is plotted as contour lines on a plane. v_α^x is the velocity of the alpha particle in frame X. Since volume is conserved under a Galilean transformation, $d^3v_\alpha^x$ and thus the quantity $d^4\sigma/d\Omega_c^{lab}d^3v_\alpha^x$ is the same independent of choice of frame. This form of data presentation has the advantage that all frames in which the correlation may be plotted are treated in a balanced way and thus the assumption that the reaction proceeds through a particular sequential break-up process is eliminated.

The in-plane and out-of-plane correlation data are plotted in the laboratory velocity space in Fig. 4a,b. The beam direction is defined to be 0 degree. The origin 0 corresponds to the

velocity of the laboratory system which is zero. The shaded circle indicates the experimental alpha energy threshold. As will be discussed in more detail later, the most probable excitation energy of $^{31}P^*$ was found to be constant at about 14.5 MeV for all the angles measured. From two-body kinematics, the velocity of $^{31}P^*$ with 14.5 MeV excitation energy can be determined and is shown by the arrow labelled v_p in the velocity plot. Circle E is centered at the recoiling velocity of $^{31}P^*$. The radius of the circle corresponds to the center of mass velocity of the alpha particle if $^{31}P^*(14.5\ MeV) \rightarrow \alpha + {}^{27}Al(g.s.)$ is assumed.

Poor statistics as well as angular interval limitations of the data set result in considerable uncertainties in the construction of the contour plot. Therefore the velocity plot gives only qualitative information. Nevertheless, the peak cross-section at all angles lies very close to circle E and can be attributed to alpha particles emitted from the recoiling $^{31}P^*$ nucleus. It can be clearly seen on the velocity plot for the in-plane data that another distinctive group of events with high alpha particle velocity appears at angles around the carbon telescope. This group of events will be discussed in more detail later.

The contours at forward angles on the opposite side of the beam from the carbon telescope are more spread out than at backward angles. In order to explore this effect quantitatively, the second moment $\langle\sigma_v^2\rangle$ of the velocity plot about the average velocity for the in-plane data are plotted in Fig. 5 as a function

of alpha angle. $\langle\sigma_v^2\rangle^{1/2}$ qualitatively corresponds to the width of the ridge in the velocity plot at a particular alpha lab angle. As can be seen in Fig. 5, $\langle\sigma_v^2\rangle$ is fairly large at the forward angles and drops by an order of magnitude at the backward angles.

The most probable carbon energy i.e. the peak of the carbon energy spectrum, is plotted in Fig. 6 as a function of alpha angle. At most angles this plot agrees with the observation by Harris el al. [1] that the most probable excitation energy of $^{31}P^*$ remains fairly constant at 14.5 MeV over all of the angles measured[1].

The contour plot for the out-of-plane data in Fig. 4b shows feature very similar to the in-plane data. From the velocity plots of Fig. 4, a majority of the events can be attributed to emission from the recoiling $^{31}P^*$ (E_x=14.5 MeV). Fig. 7 shows the in-plane and out-of-plane C–α angular correlation function plotted in the center of mass frame of $^{31}P^*$. Note that the recoil direction of $^{31}P^*$ is defined to be zero degrees in the center of mass system of $^{31}P^*$. The C–α angular correlation reaches a minimum about 90° and rises at backward angles. Two main features observed, the forward angle peaking and a backward angle rise in the C–α angular correlation are in disagreement with the results of Harris et al.[1]. The earlier results indicated that the C–α angular correlation was peaked along the recoil direction of $^{31}P^*$ and continued to decrease at backward angles past 90° in the center of mass system of $^{31}P^*$. For comparison, results from this work and from that of Harris et al. are plotted in Fig. 1. The

discrepancy at the backward angles may in part be explained by the fact that the DE detector of the alpha telescope used in the earlier experiment was 12μ thick. A 12μ thick DE detector will range out alpha particles with energy less than 3 MeV. The time of flight method used in this work has no such cutoff problem. No satisfactory answer seems to explain the discrepancy which exists at the forward angles. During the course of this work, measurements at these forward angles have been repeated several times with both the two-telescopes method and the TOF method with reproducible results. The discrepancy with the earlier work[1] persists.

The out-of-plane C-α correlation function as shown in Fig. 7b drops to a minimum at about 90° which is much lower in cross-section than the minimum of the in-plane C-α correlation in Fig. 7a. Past $\phi_{\alpha}=90^{\circ}$, the C-α angular correlation rises up again. Thus, the out-of-plane data obtained indicates peaking in the reaction plane.

V. Discussion

One of the goals of this work is to understand the nature of the pre-equilibrium alpha emission process. In order to extract the pre-equilibrium component, all other processes that contribute to the alpha emission should be identified and subtracted.

1. Break Up Events from $^{16}O^{*}$:

The in-plane velocity plots of $\theta_c=-30^{\circ}$ data shown in Fig. 4a suggests that there are at least two groups of events, one

that lies near the circle E which is centered on the velocity of the recoiling nucleus $^{31}P^*$ and another group with high alpha energy and low carbon energy around the carbon telescope. This latter group is observed only at $\theta_\alpha=-17^\circ$ and -43°. The two-dimensional plot of E_c vs. E_α for $\theta_c=-30^\circ$ and $\theta_\alpha=-17^\circ$ is shown in Fig. 8. Since the second group of events seem to occur only around the carbon detector, this leads to the conclusion that these events probably arise from the break up of the inelastically scattered $^{16}O^*$. Such a mechanism can be represented as follows :

$$^{16}O + {}^{27}Al \rightarrow {}^{27}Al + {}^{16}O^*$$

$$^{16}O^* \rightarrow \alpha + {}^{12}C$$

The ^{16}O break up process has been observed by Ho et al.[6] in the $^{58}Ni + {}^{16}O$ system at 92 MeV and more recently by Sasagase et al for the $^{27}Al + {}^{16}O$ system at 88 MeV[10].

From the carbon and alpha energies of this group of events with high alpha energy and low carbon energy, one can deduce the excitation energy of oxygen to be between 9.5 to 11 MeV. If one examines the energy level diagram of ^{16}O, the lowest energy level in ^{16}O that can decay by alpha emission is at 9.63 MeV. Proton decay starts to compete with the alpha decay above 12.1 MeV. The solid triangle indicates the double differential cross-section at $\theta_\alpha=-17^\circ$ after the ^{16}O break up events have been subtracted. The large uncertainties come from the lack of information about the differential cross-section for the production of the $^{16}O^*$. The upper limit is obtained by assuming that only the group of events with low carbon energy and high alpha energy shown in Fig. 8 is

subtracted. This upper limit is given by the upper part of the error bar.

2. Equilibrium Contribution :

The majority of the events shown in the velocity plots (Fig. 4a,b) are consistent with the assumption that the alpha particles are emitted from the intermediate nuclei $^{31}P^*$. One would expect that equilibrium evaporation from $^{31}P^*$ will contribute to alpha particle emission. Ericson and Strutinsky[18] first showed that evaporation from a rotating nucleus can be treated classically. Halpern has developed a classical model for emission from a spherical rotating Maxwell gas[19]. Part of this model was reproduced by Gruhn in his thesis[20]. If a rotating nucleus is assumed to rotate around an axis that is perpendicular to the reaction plane, then one would expect the angular distribution of evaporated particles to be isotropic in the equatorial plane. Owing to the centrifugal force, the yield is concentrated in the equatorial plane and decreases as one goes towards the pole. If the rotating axis is normal to the reaction plane, then the equatorial plane is the reaction plane.

The yield of evaporation particles as a function of polar angle Ψ defined with respect to the axis of rotation is given by Halpern as:

$$Y(\Psi)=Y_o \exp(X*\sin^2\Psi) \qquad (1)$$

where Y_o is the normalization factor and X is the ratio of rotational kinetic energy to the thermal nuclear energy. The

ratio X is given by :

$$X = .5\mu R^2 \omega^2/(2T)$$

2

where μ is the reduced mass, ω is the angular velocity, T is the nuclear temperature, and R is the distance of the alpha particles from the residual nucleus. For the distance R, the following equation

$$R = 1.25(A_{\alpha}^{1/3} + A_{Al}^{1/3})$$

is used.

X can also be expressed in terms of the spin (J) of the rotating nucleus.

$$X = .5(J+1/2)^2/(2IT)$$

3

where $I=\mu R^2$ is the moment of inertia.

From the excitation energy of $^{31}P^*$, one can estimate the temperature with an empirical formula[21]

$$E=aT^2$$

4

For the most probable excitation energy of $^{31}P^*$ of 14.5 MeV, the corresponding temperature is found to be 1.9 MeV.

Suppose the z axis is defined to be normal to the reaction plane. Perfect alignment of the rotational axis along the z axis is expected only if the ^{16}O projectile is treated as a point object. In this case, the alpha particle that was transferred from ^{16}O to ^{27}Al lies in the equatorial plane of the ^{27}Al. Since both $\vec{r}_{\alpha}$ and $\vec{p}_{\alpha}$ lie in the equatorial plane, then the angular

momentum transferred $\vec{\ell}_\alpha = \vec{r}_\alpha \times \vec{p}_\alpha$ is normal to the reaction plane.

In reality, the oxygen nucleus has finite size, thus the alpha particle can be transferred slightly above and below the equatorial plane. However the average momentum transferred by the alpha particle is expected to lie in the reaction plane near the recoil direction of the composite nucleus $^{31}P^*$. The angular momentum of the $^{31}P^*$ then lies in the plane perpendicular to the momentum transfer direction.

From the argument described above, the recoil direction is taken to be the momentum transfer direction. This choice of momentum transfer axis is partly guided by the experimental data as the in-plane angular correlation exhibits a minimum around 90^o in the $^{31}P^*$ center of mass system. Experimentally, for sequential decay the momentum transfer direction has been found to lie very close to the recoil direction of the intermediate nucleus[22]. Furthermore, the minimum of the angular correlation cannot be determined to an accuracy of better than 30^o from the present data. Thus the above assumption would not greatly affect the contribution from equilibrium evaporation obtained using the formalism described.

The angle between the rotational axis and the z axis is defined to be γ. The coordinate system used is shown in Fig. 9. It is chosen to simplify the evaporation analysis and differs from that often used.

In order to estimate the contribution of the evaporation component in a simple way, γ is assumed to be gaussian

distributed. A similar formalism has been employed by Dyer et al.[23] to describe the in-plane and out-of-plane angular correlation of fission fragments from sequential decay of heavy nuclei in deeply inelastic collisions.

From Equation 1, the angular distribution is

$$W(\theta,\phi) = \int d\beta \exp[-\beta^2/2\beta_o^2] Y(\Psi) \qquad 5$$

where Ψ is related to the angles β, θ, and ϕ shown in Fig. 9 by the cosine law:

$$\cos\Psi = \cos\beta\cos\phi + \sin\beta\sin\phi\sin\theta \qquad 6$$

The angular distribution $W(\theta,\phi)$ used in Equation 5 is the same as the experimental quantity $(d^2\sigma/d\Omega_c d\Omega_\alpha)^{cm}$. In order to emphasize the θ and ϕ dependence of this quantity, the more convenient notation $W(\theta,\phi)$ is adopted.

Both the out-of-plane data and the in-plane data are used to fit the three parameters β_o, X and Y_o. The solid lines in Figs. 7a,b are the best fit for the in-plane and out-of-plane data at $\theta_c = -30^o$ obtained by using only backward angle ($\theta_\alpha^{cm} > 90^o$) in-plane data along with the out-of-plane data since the evaporative component is expected to dominate at backward angles. Only the in-plane data from $-30^o < \theta_\alpha^{cm} < 0^o$ are not fit by this purely evaporative model. All other angles are seen to be fit very well by the simple evaporative angular correlation. Best χ^2 values for β_o, X and Y_o are found to be 28^o, 2.6 and 110μb/sr^2 respectively.

Since β_o is a measure of dealignment of the rotational axis

along the z axis normal to the reaction plane, the value $\gamma_o = 28^o$ means that the dealignment is small. The rotational axis lies very close to the z axis. Following the argument on the angular momentum transfer by the alpha particle described above, one can obtain a very rough geometric estimate of the maximum value of γ by taking the inverse tangent of the ratio $R_{c-\alpha}/R_{c-Al}$ where R_{i-j} is the optical potential radius given by

$$R_{i-j} = 1.25(A_i^{1/3} + A_j^{1/3}).$$

γ_{max} is found in this manner to be around 36^o. Thus the value of γ_o obtained from fitting the experimental data is within the limits of what one expects from a simple geometric argument. It is also interesting to note that γ_o obtained in the present work is very close in value to the dealignment factor obtained by Dyer et al.[23] in describing the fission fragments from heavy product nuclei.

From the value obtained for X, one can estimate the mean spin of the rotating nucleus to be $\langle J \rangle \sim 7\hbar$ using Equations 3 and 4. Since the measured alpha decay from the $^{31}P^*$ nucleus leaves the ^{27}Al in the ground state, the statistical model employed is not strictly applicable. Thus the value of $\langle J \rangle$ deduced has only qualitative significance. It is however very close to that expected for an (^{16}O, ^{12}C) alpha transfer reaction.

In addition, the differential cross-section leading to alpha evaporation can be calculated with following equation :

$$(d\sigma/d\Omega_c)_{ev} = \int_o^{\pi} \sin\phi d\phi \int_o^{2\pi} d\theta W(\theta,\phi)$$

$(d\sigma/d\Omega_c)_{ev}$ is found to be $790\ ^{+125}_{-75}$ μb/sr. One can estimate $(d\sigma/d\Omega_c)$ from the experimental carbon singles data. This is found to be 6.5 mb/sr. Thus the ratio $(d\sigma/d\Omega_c)_{ev}/(d\sigma/d\Omega_c)$ is about .012. This result is consistent with that obtained from a statistical calculation.

3. Pre-equilibrium Contribution

The pre equilibrium alpha emission contribution is operationally defined here to be the experimental yield minus the yield from evaporation and from the break up of $^{16}O^*$. It is plotted in the center of mass frame of $^{31}P^*$ in Fig. 10. The corresponding lab angles are given on the top axis. Since the value of the Jacobian does not change very much over this range, the pre-equilibrium component would show very similar features in the lab frame.

a. Differential Cross-Section:

The pre-equilibrium differential cross-section can be obtained by integrating the in-plane and out-of-plane angular correlation of the pre-equilibrium component. However, the out-of-plane angular correlation was measured for only a single in-plane projection angle. This correlation indicates that the total alpha emission cross-section concentrates in the reaction plane. There is no quantitative out-of-plane information for the pre-equilibrium component. Nevertheless, one can use the available experimental information to make a rough estimate of the

pre-equilibrium component contribution to C-α coincident events. It is assumed that the ϕ (out-of-plane) dependence of the pre-equilibrium angular distribution is the same as the ϕ dependence of the equilibrium angular distribution, leading to

$$W_{pre}(\theta,\phi) = [W_{pre}(\theta,90^{o})/W_{eq}(\theta,90^{o})]\cdot W_{eq}(\theta,\phi) \qquad (9)$$

where $W_{pre}(\theta,90^{o})$ is the extracted in-plane correlation function for the pre-equilibrium component as shown in Fig. 10 and $W_{eq}(\theta,90^{o})$ is given by the best-fit solid curve shown in Fig. 7a. The assumption used probably overestimates the contribution of the pre-equilibrium differential cross-section. Experimentally, as will be discussed later, the average alpha energy for the pre-equilibrium component is higher than the equilibrium component. Thus one would expect the angular momentum for pre-equilibrium alphas to be higher than the equilibrium alphas and the ϕ dependence of the pre-equilibrium angular distribution might be steeper than that of the equilibrium component.

With the above assumption, one then obtains the ratio of the pre-equilibrium contribution to the equilibrium contribution from the in-plane angular distribution,

$$\frac{(d\sigma/d\Omega_{c})_{pre}}{(d\sigma/d\Omega_{c})_{eq}} = \frac{\int d\Omega W_{pre}(\theta,\phi)}{\int d\Omega W_{eq}(\theta,\phi)} \simeq .1 \qquad (10)$$

The exact value of $(d\sigma/d\Omega_{c})_{pre}$ depends on the exact ϕ dependence of $W_{pre}(\theta,\phi)$ and the exact shape of the dashed line shown in Fig. 10 where no experimental data is available. The

exact value of $(d\sigma/d\Omega_c)_{pre}$ is not important for our present purpose. What this analysis shows is that the pre-equilibrium component is small compared to the equilibrium one.

The break-up of $^{16}O^*$ contributes a very small fraction of the total C-α coincidence events detected experimentally and can be neglected in the deduction of the fraction of events associated with pre-equilibrium emission. From the above analysis, the pre-equilibrium component contributes about 10% of the total C-α coincidence events detected experimentally. For the system of $^{27}Al + ^{16}O$ at 65 MeV, pre-equilibrium alpha emission is not the dominant mechanism for producing alpha particles in coincidence with carbon particles as suggested previously[1].

b. Mean Alpha Energy:

The mean alpha energy in the center of mass frame of $^{31}P^*$, $\langle E_\alpha^{cm} \rangle$, is plotted as a function of alpha angle in Fig. 11. The data points at the most backward alpha angles were excluded since they suffer from the low alpha energy cutoff problem arising from very low energy alpha particles ranging out in the target or falling below the detector threshold. Over most angles, $\langle E_\alpha^{cm} \rangle$ is constant as expected if the alpha particles come from the evaporation of $^{31}P^*$. For the forward angles where the pre-equilibrium alpha emission is important, $\langle E_\alpha^{cm} \rangle$ is much higher than obtained at the back angles. The mean alpha energy of the pre-equilibrium component for each alpha angle can be estimated in the following way :

$$\langle E_\alpha^{cm} \rangle = f \times \langle E_\alpha^{cm} \rangle_{pre} + (1-f) \times \langle E_\alpha^{cm} \rangle_{eq}$$

where f is the fraction of pre-equilibrium alpha particles emitted. $\langle E_\alpha^{cm} \rangle_{eq}$ is the average energy for the equilibrium component and can be determined from Fig. 11 to be $5.2 \pm .5$ MeV. $\langle E_\alpha^{cm} \rangle_{pre}$ is the average energy for the pre-equilibrium alphas and can be determined from Equation 11 to be 8 ± 2 MeV. The large error in $\langle E_\alpha^{cm} \rangle_{pre}$ is mainly due to the uncertainty in determining f. The average alpha lab energy for the pre-equilibrium component is estimated to be 15 ± 3 MeV. The corresponding velocity of the pre-equilibrium alpha particles is comparable to the beam velocity.

The pre-equilibrium alpha energy spectrum for these forward angles are broadly distributed from 7 to 24 MeV in the lab reflecting the broadening of the velocity contour plots at the forward angles as shown in Fig. 4a. It was shown earlier that the most probable excitation energy of $^{31}P^*$ remained constant for most angles measured. This merely reflects the fact that the contribution from the evaporation of $^{31}P^*$ (E_x=14.5 MeV) is very important even at forward angles. There is no strong experimental evidence to support the assumption that the pre-equilibrium component comes from sequential decay of $^{31}P^*$ as suggested previously[1].

VI. Summary

The results from the present work can be summarized as follows :

1. At $\theta_c=-30^o$, the majority of C-α coincidence events come from evaporation of $^{31}P^*$. A small number of alpha particles from the break up of $^{16}O^*$ are detected at angles around the carbon detector. Less than 10% of the alpha particles detected are of pre-equilibrium origin.

2. The pre-equilibrium alpha particle angular correlation does not peak along the recoil direction as was previously reported[1]. It continues to rise to the smallest angle measured on the opposite side of the beam direction as the carbon detector.

3. The average velocity of the pre-equilibrium alpha particles is about the same as the beam velocity and the energy is much higher than the energy of equilibrium alphas.

4. The present work does not give enough information to establish the mechanism for producing pre-equilibrium alphas. Measurements at smaller angles with respect to the beam would be highly desirable.

VII Concluding Remarks

The results obtained from the present experiment and the earlier results obtained by Harris et al.[1] differ significantly. The earlier results of a peaking along the recoil direction and a falloff past 90^o in the recoil frame supported the hypothesis that pre-equilibrium sequential alpha decay from an intermediate nucleus $^{31}P^*(E_x=14.5$ MeV) was the dominant mode of alpha emission. The results from the present work, especially the experimental evidence from the out-of-plane angular correlation and in-plane

back angle data, indicate that the C-α coincident events observed mainly come from equilibrium alpha evaporation from the intermediate nucleus $^{31}P^{*}(E_x=14.5$ MeV). More recent results from other systems[7,24] also indicate that contributions due to alpha evaporation, either from the projectile-like or target-like particles, are very important and in most cases account for nearly all of the heavy-ion, alpha coincidence events observed. It is important to establish the properties of the evaporative component in order to enable the proper extraction of the smaller pre-equilibrium component.

REFERENCES

* Work supported by U.S. Department of energy.

1. J.W. Harris, T.M. Cormier, D.F. Geesaman, L.L. Lee, Jr., R.L. McGrath, and J.P. Wurm, Phys. Rev. Lett.28, 1460 (1977).

2. J.W. Harris, P. Braun-Munzinger, T.M. Cormier, D.F. Geesaman, L.L. Lee, Jr., R.L. McGrath and J.P. Wurm, Proc. Internat. Conf. Nucl. Structure, Tokyo, (1977) p. 698.

3. A. Gamp, J.C. Jacmart, N. Poffe, H. Doubre, J.C. Roynette, and J. Wilczynski, Phys. Lett.74B, 215 (1978).

4. G.K. Gelbke, M. Bini, C. Olmer, D.L. Hendrie, J.L. Laville, M. Mahoney, M.C. Mermaz, D.K. Scott and H.H. Wieman, Phys. Lett. 71B, 83 (1977).

5. T. Shimoda, M. Ishihara, H. Kamitsubo, T. Motobayashi, and T. Fukuka, Proc. IPCR Symp. on Macroscopic Features of Heavy Ion Collisions and Pre-Equilibrium Process, Hakone (1977) p. 93.

6. H. Ho, R. Albrecht, D. Dunnweber, G. Graw, S.G. Steadman, J.P. Wurm, D. Disdier, V. Rauch and F. Scheibling, Z. Phys. A283, 237 (1977).

7. R.K. Bhowmik, E.C. Pallocco, N.E. Sanderson, J.B.A. England and G.C. Morrison, Phys. Lett. 80B, 41 (1978).

8. A. Gamp, H.L. Harney, J.C. Jacmart and N. Poffe, Z. Phys. A291,347 (1979).

9. R. Billerey, C. Cerutti, A. Chevarier, N. Chevarier, B. Cheynis, and A. Demeyer, Z. Phys. A292, 293 (1979).

10. M. Sasagase, M. Sato, S. Hanashima, K. Furuno, Y. Tagishi, Y. Nagashima, S.M. Lee and T. Mikumo, Proceedings of International Conference on

Nuclear Physics, Berkeley, California, 1980, p. 527.

11. D.H.E. Gross and J. Wilczynski, Phys. Lett. 67B, 1 (1977).

12. P.A. Gottschalk and M. Westrom, Nucl. Phys. A314, 232 (1979).

13. K. Siwek-Wilczynska, E.M. du Marchie van Voorthuysen, J. van Popta, R.H. Siemssen and J. Wilczynski, Phys. Rev. Lett. 42, 1599 (1979).

14. J.R. Wu and T.Y. Lee, Phy. Rev. Lett. 45, 8 (1980).

15. F.C. Shoemaker, J.E. Faulkner, G.M.B. Bouricius, S.G. Kaufmann, and F.P. Mooring, Phys. Rev. 83, 1011 (1951).

16. C.W. Reich, G.C. Phillips and J.R. Russell, Jr., Phys. Rev. 104, 143 (1956).

17. P. Genthier, H. Ho, M.N. Namboodiri, J.B. Natowitz, L. Alder, O. Hartin, P. Kasinaji, A. Khodai, S. Simon, and K. Hagel, Texas A & M Cyclotron Institute Progress Report (1979), pg. 7.

18. T.E.O. Ericson and V.M. Strutinski, Nucl. Phys. 8, 284 (1958) 9, 689 (1959).

19. I. Halpern, Bull. Amer. Phys. Soc. II, 5, 510 (1960) and private communication.

20. C. Gruhn, Thesis, University of Washington, Seattle, 1961.

21. R.R. Roy and B.P. Nigam in Nuclear Physics, John Wiley and Sons, Inc., p. 206.

22. H. Eichner, H. Stehle and P. Heiss, Nucl. Phys. A205,249 (1973).

23. P. Dyer, R.J. Puigh, R. Vandenbosch, T.D. Thomas, M.S. Zisman, and L. Nunnelley, Nucl. Phys. A322, 205 (1979).

24. M.N. Namboodiri and J.B. Natowitz, private communication on the system $^{20}Ne + ^{27}Al$ at 120 MeV.

LIST OF FIGURES

Fig. 5 The second moment of the velocity plot plotted as a function of the alpha lab angle for the in-plane data, $\theta_c=-30^o$. See Fig. 1 for explanation of symbols.

Fig. 6 The most probable carbon energy plotted as a function of in-plane alpha angles for $\theta_c=-30^o$.

Fig. 7 C-α angular correlation function in the center of mass system of $^{31}P^*$ (E_x=14.5 MeV), $\theta_c=-30^o$ (a) in-plane data, (b) out-of-plane data. See Fig. 1 for explanation of symbols for the data points. The solid triangle is obtained when the contribution due to break-up of $^{16}O^*$ is subtracted. the solid curve is the best fit of Equation 5. The dashed curves indicates the upper and lower limit by adjusting the normalization constant Y_o of Equation 1.

Fig. 8 Two dimensional plot of the number of counts as a function of E_c and E_α for $\theta_c=-30^o$, $\theta_\alpha=-17^o$.

Fig. 9 Coordinate system used in describing a rotating $^{31}P^*$ nucleus emitting an alpha particle. The reaction plane is defined by the beam and the carbon detector.

Fig. 10 Extracted pre-equilibrium alpha double differential cross-section plotted as a function of alpha angle for $\theta_c=30^o$ in the $^{31}P^*$ center of mass system. The corresponding lab angles are also given at the top of the figure.

Fig. 11 Mean α energy plotted as function of α angle in the $^{31}P^*$ center of mass system. The straight line denotes $\langle E_\alpha^{cm} \rangle=5.2$ MeV.

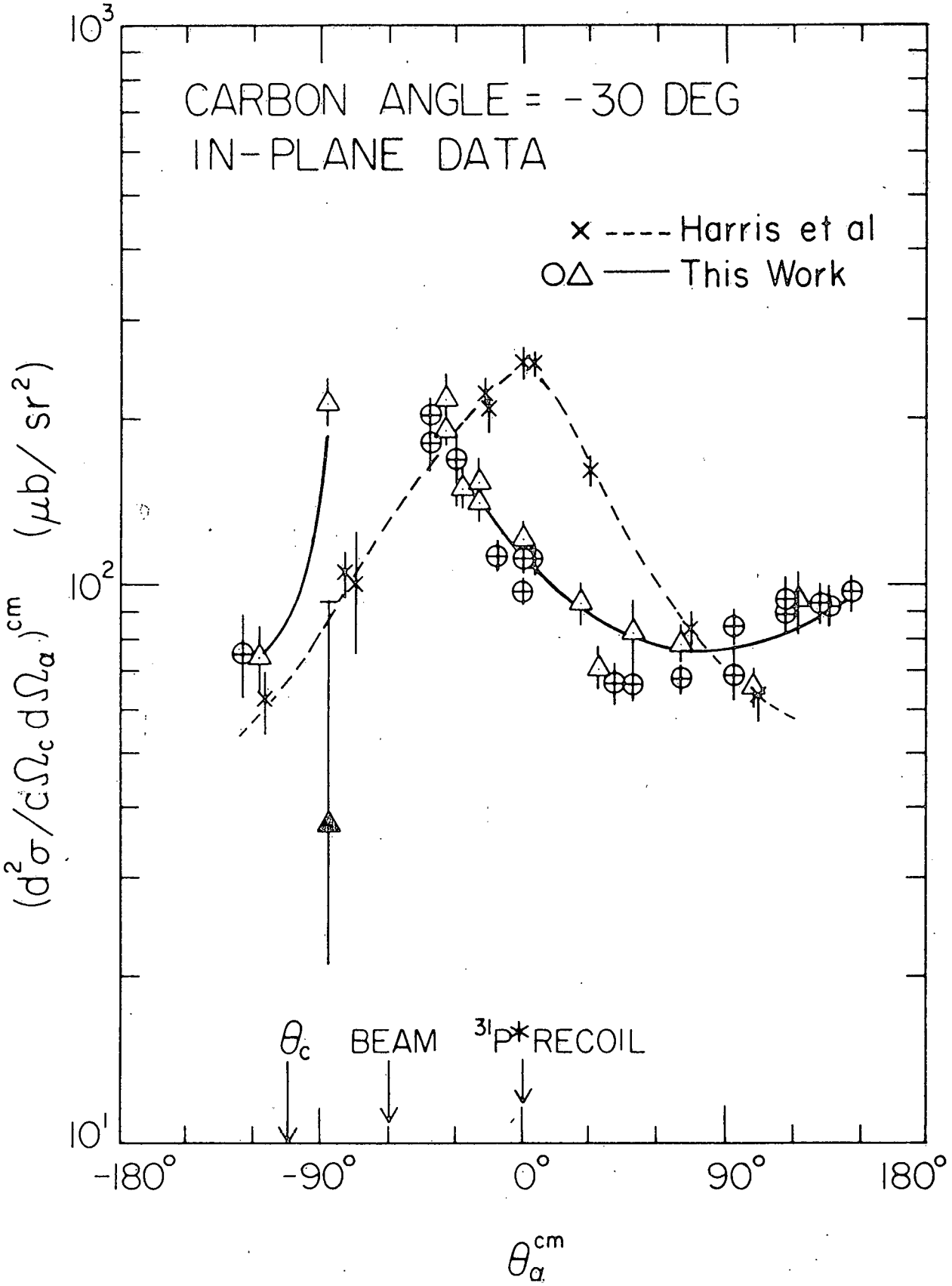
CARBON ANGLE = -30 DEG
IN-PLANE DATA
× ---- Harris et al
○△ —— This Work
10^3
10^2
10^1
$(d^2\sigma/c\Omega_c d\Omega_\alpha)^{cm}$ $(\mu b/sr^2)$
θ_c
BEAM
$^{31}P^*$ RECOIL
-180°
-90°
0°
90°
180°
θ_α^{cm}

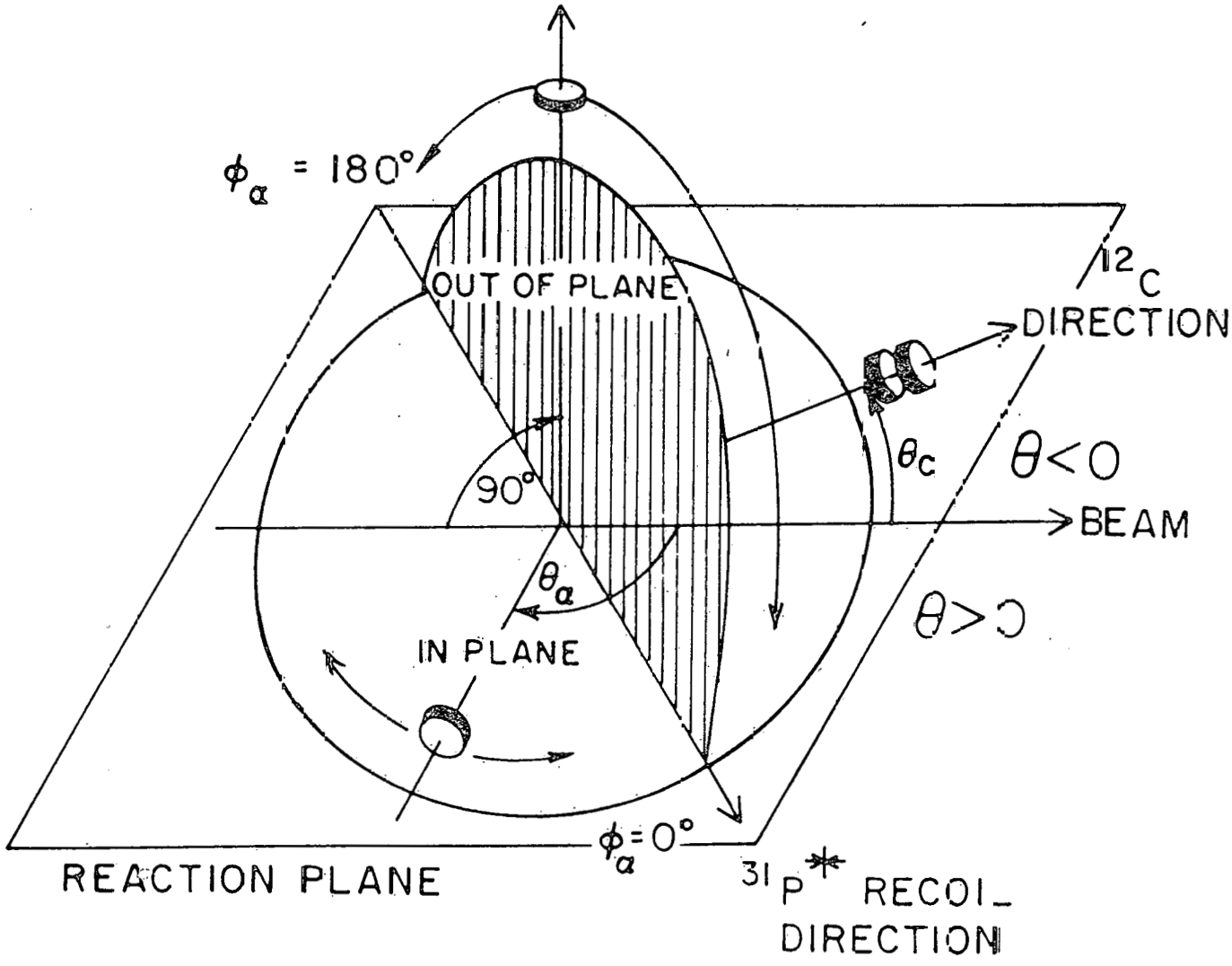
ϕ_α = 180°
OUT OF PLANE
^{12}C DIRECTION
θ_c
$\theta<0$
90°
BEAM
θ_α
$\theta>0$
IN PLANE
ϕ_α=0°
REACTION PLANE
$^{31}P^*$ RECOIL DIRECTION

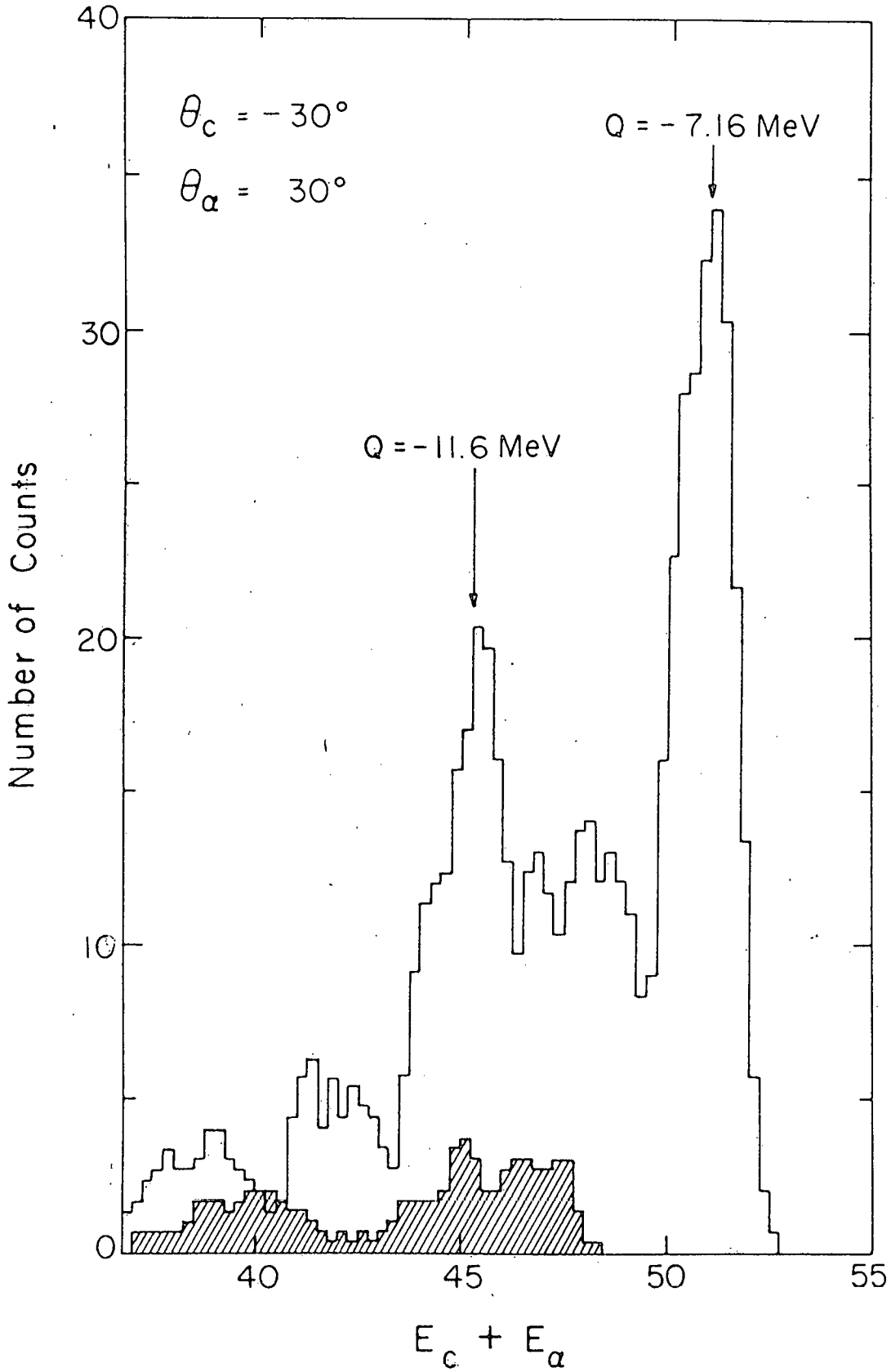
40
30
20
10
0
$\theta_c = -30°$
$\theta_\alpha = 30°$
Q = - 7.16 MeV
Q = - 11.6 MeV
Number of Counts
40
45
50
55
$E_c + E_\alpha$

$\theta_c = -30°$
IN-PLANE DATA

——— 1 cm/ns

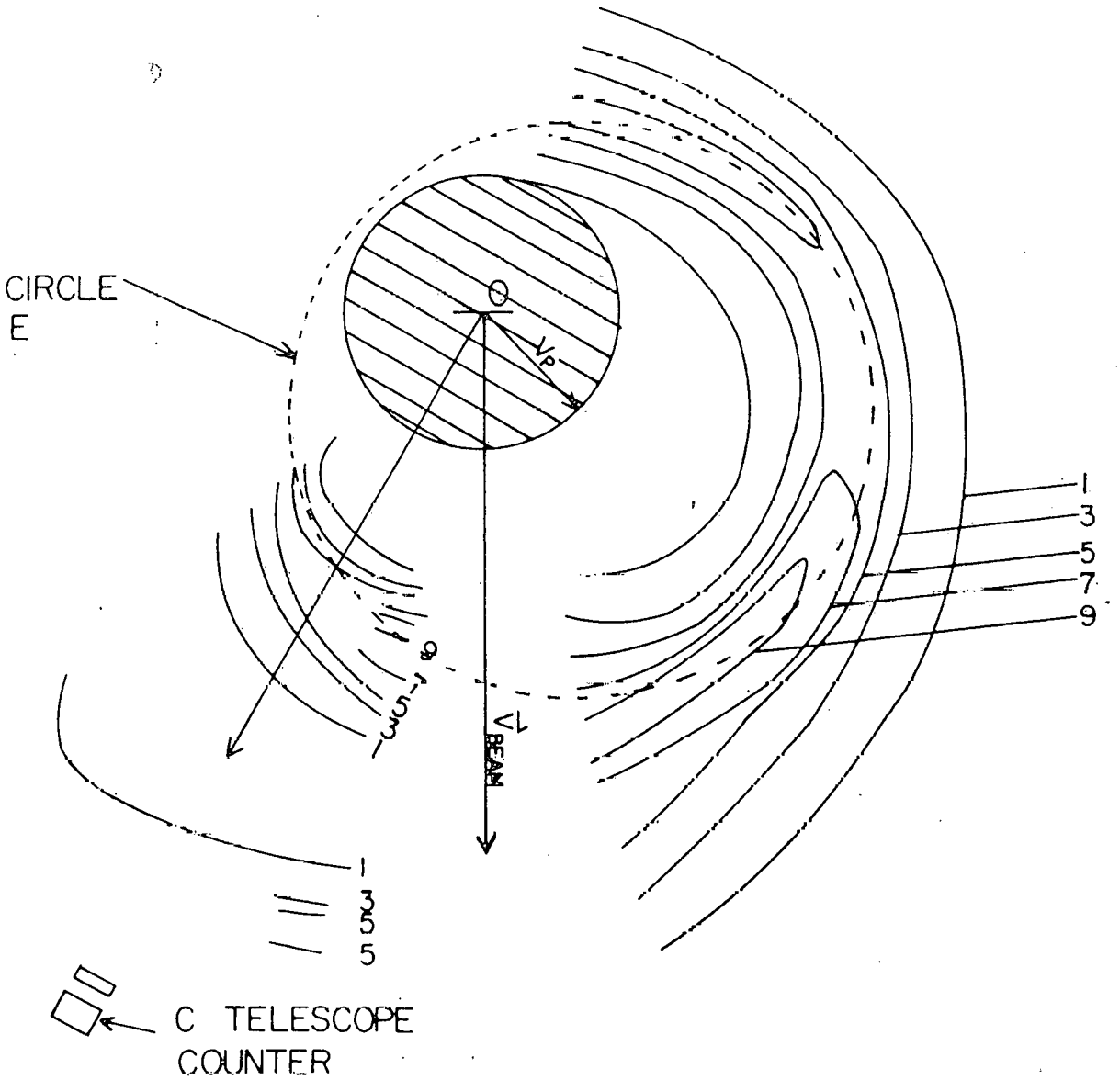

$\theta_c = -30°$
OUT-OF-PLANE DATA

——— 1 cm/ns

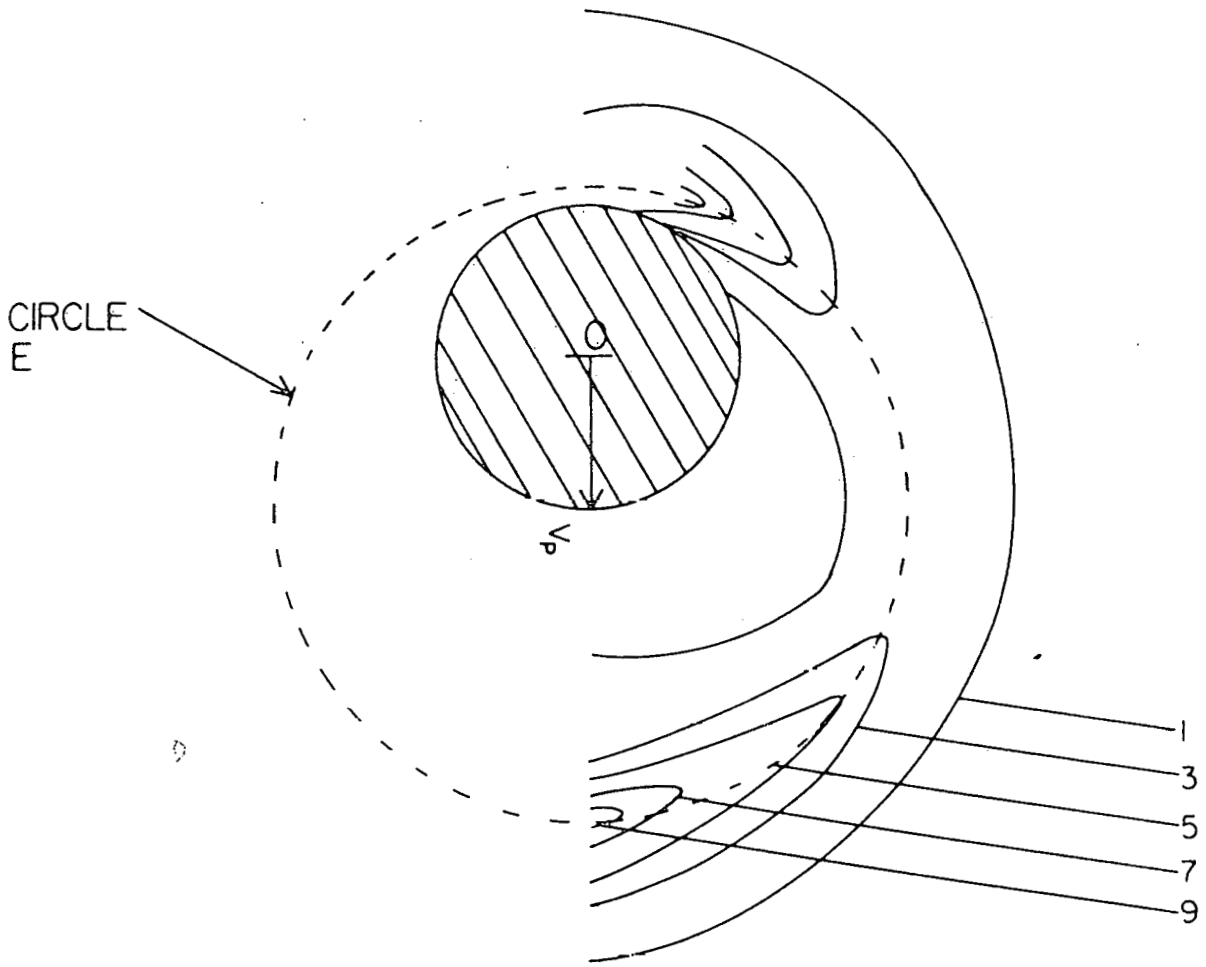

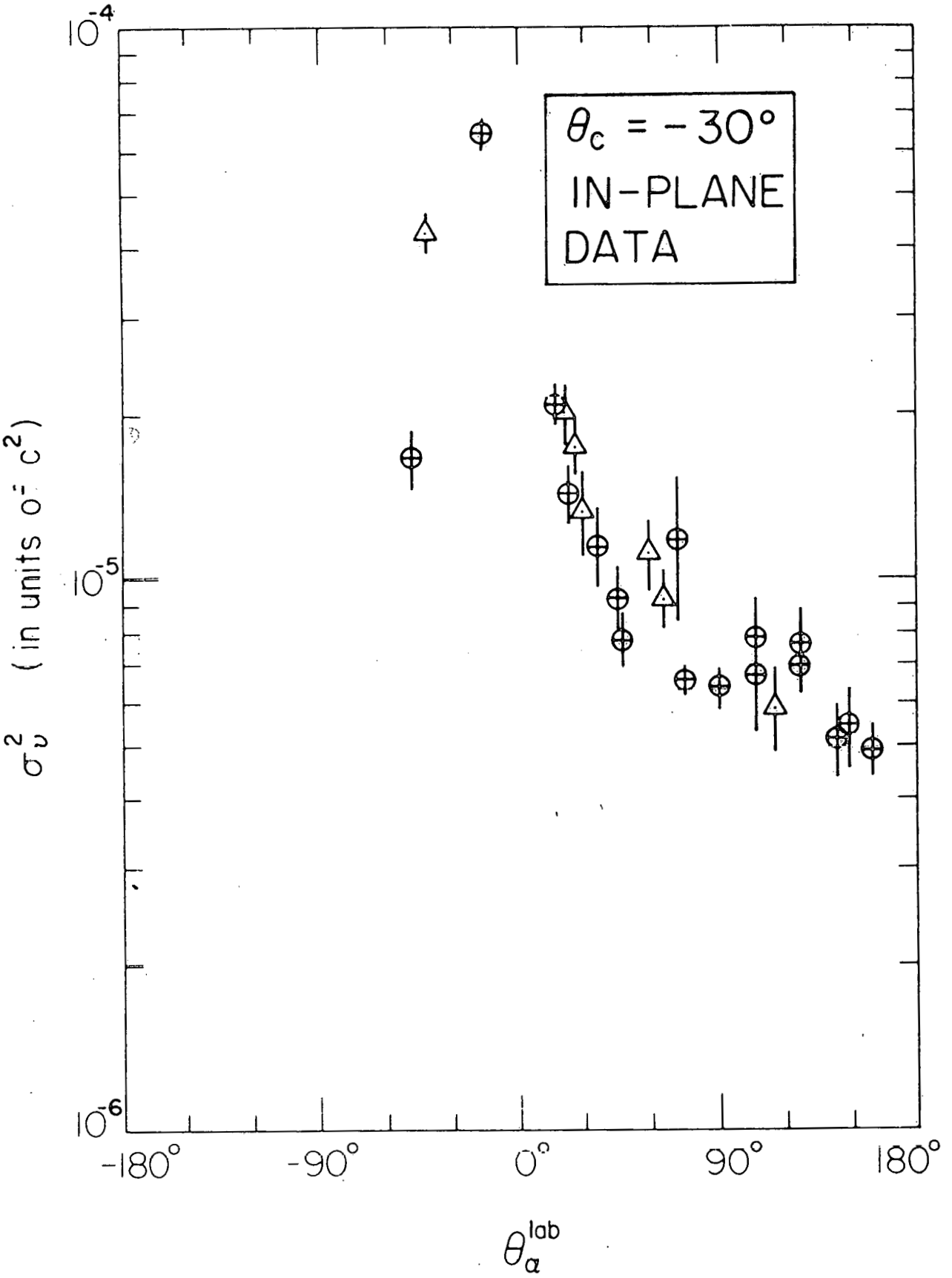
$\theta_c = -30°$
IN-PLANE
DATA
10^{-4}
10^{-5}
10^{-6}
σ_ν^2 (in units of c^2)
-180°
-90°
0°
90°
180°
θ_α^{lab}

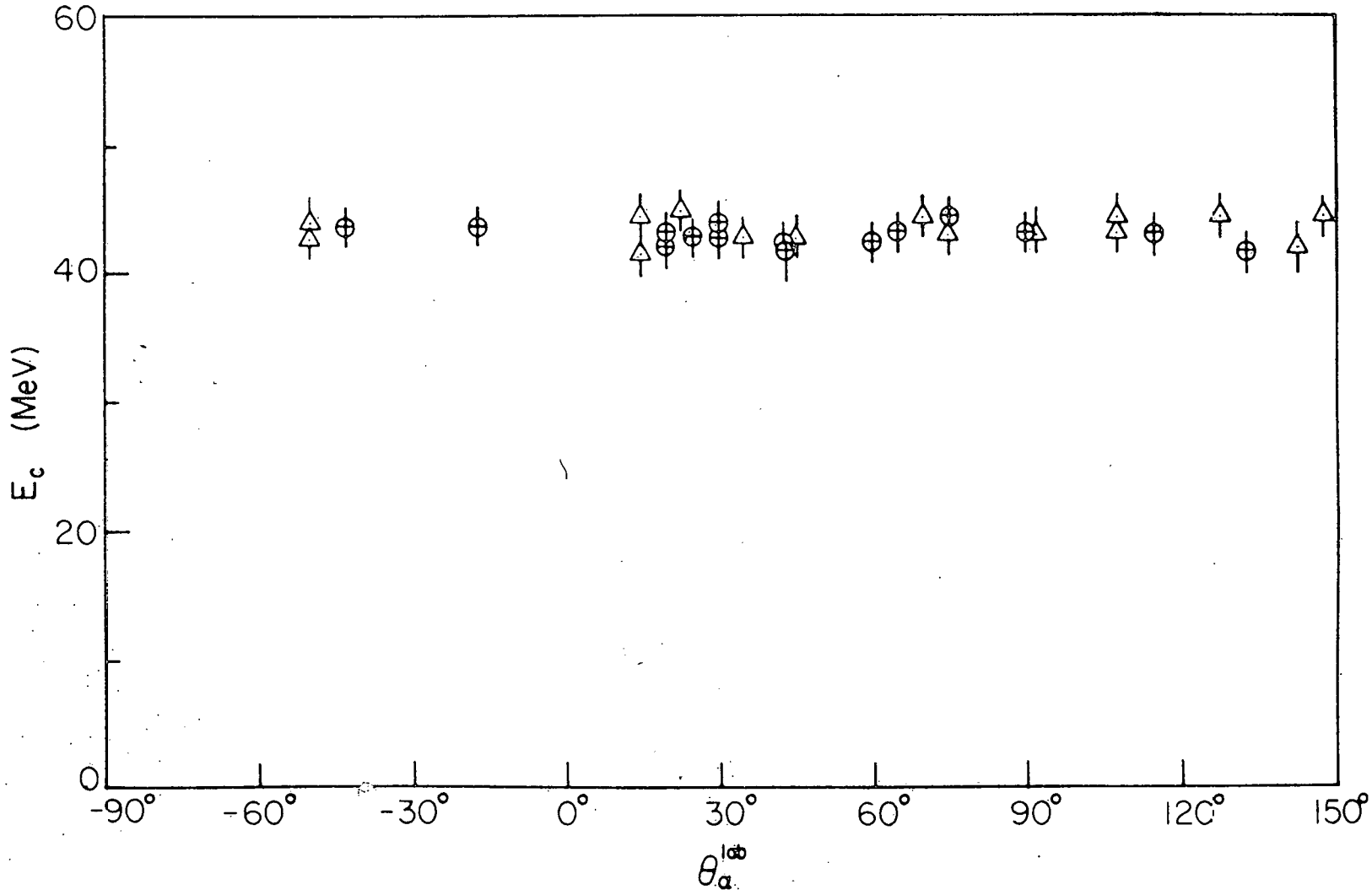
60
40
20
0
E_c (MeV)
-90°
-60°
-30°
0°
30°
60°
90°
120°
150°
θ_α^{lab}

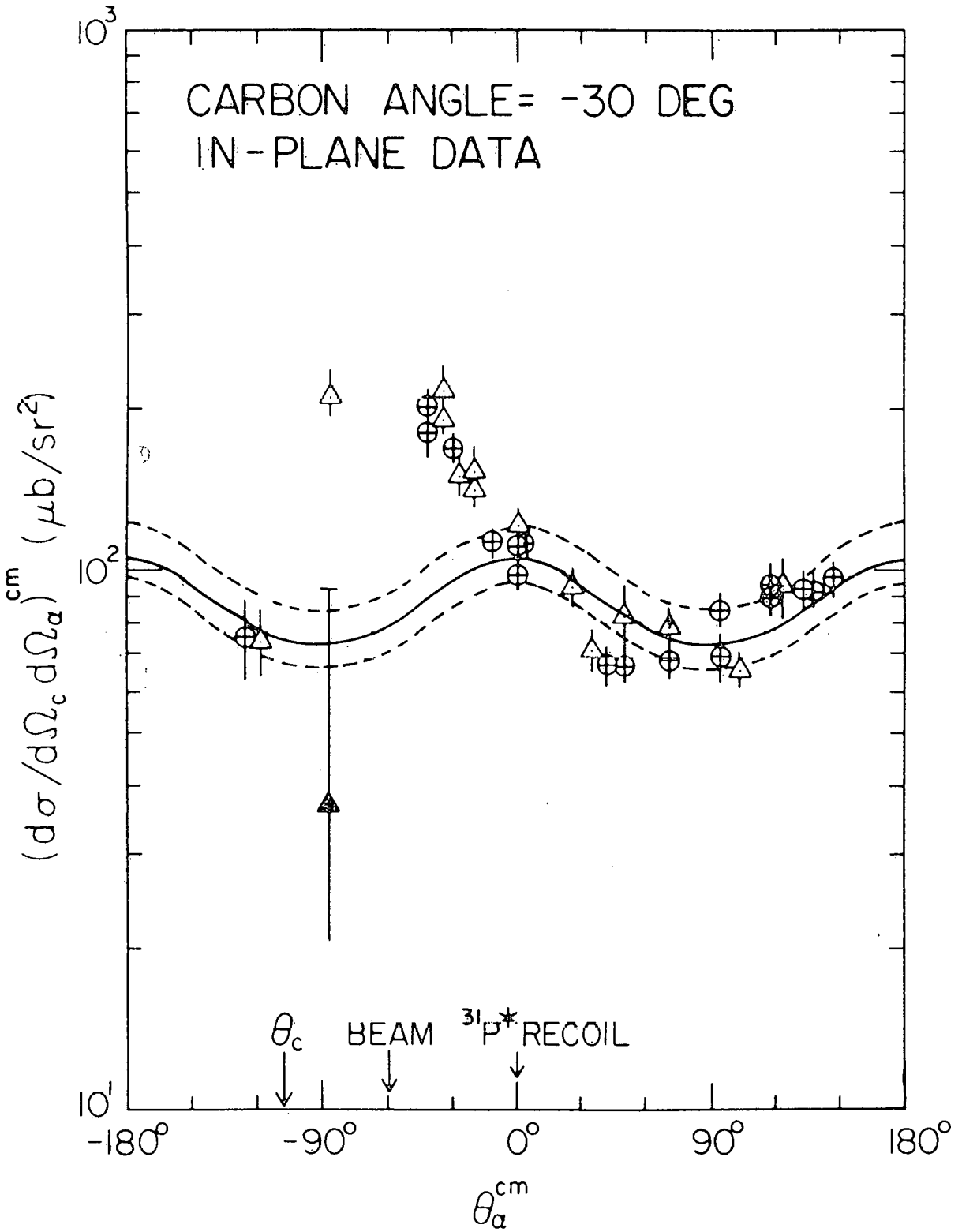
CARBON ANGLE= -30 DEG
IN-PLANE DATA
10^3
10^2
10^1
$(d\sigma/d\Omega_c\, d\Omega_\alpha)^{cm}$ (μb/sr^2)
θ_c
BEAM
^{31}P* RECOIL
-180°
-90°
0°
90°
180°
θ_α^{cm}

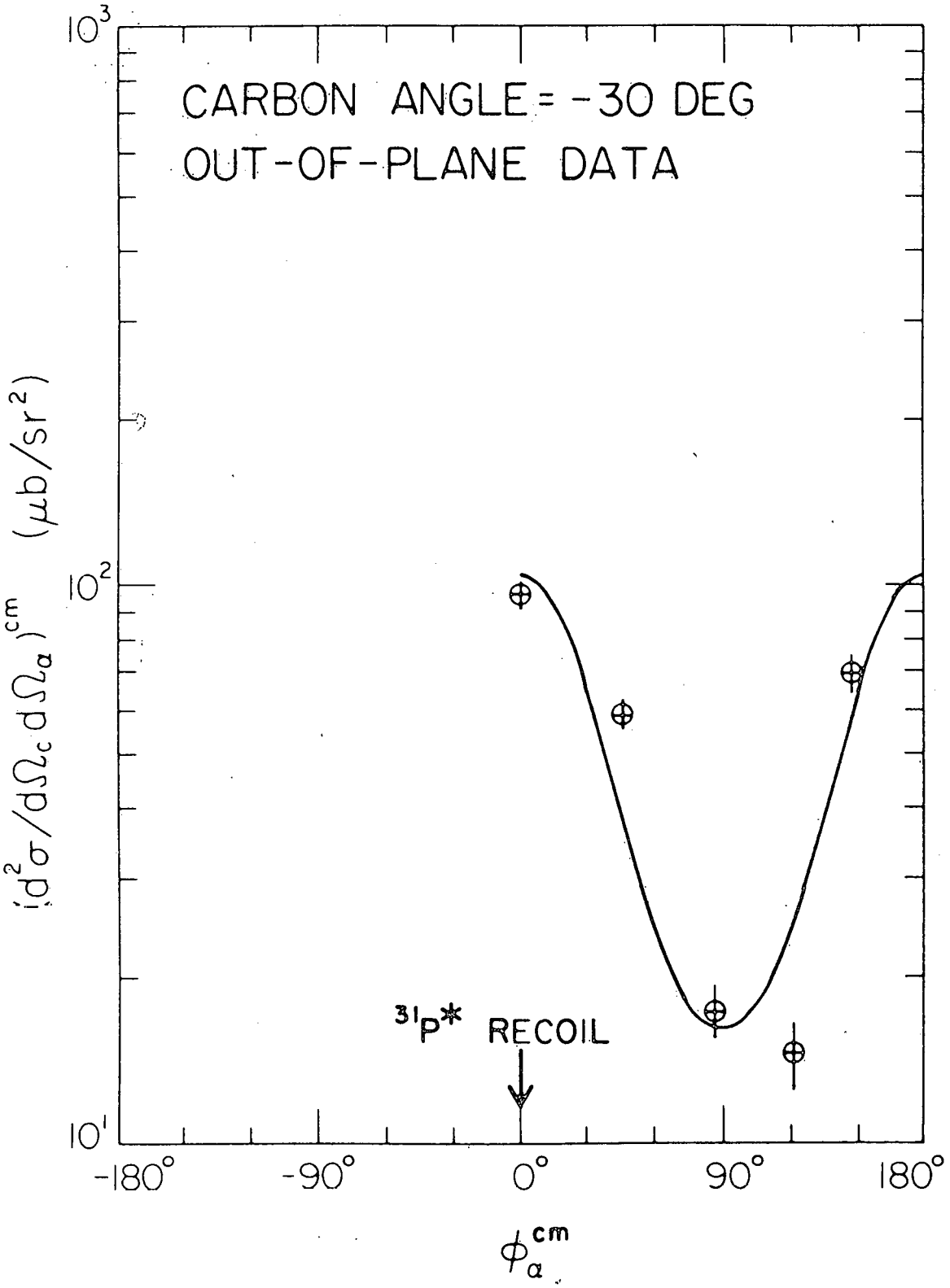
CARBON ANGLE = -30 DEG
OUT-OF-PLANE DATA
10^3
10^2
10^1
$d^2\sigma/d\Omega_c\, d\Omega_\alpha)^{cm}$ (μb/sr^2)
^{31}P* RECOIL
-180°
-90°
0°
90°
180°
ϕ_α^{cm}

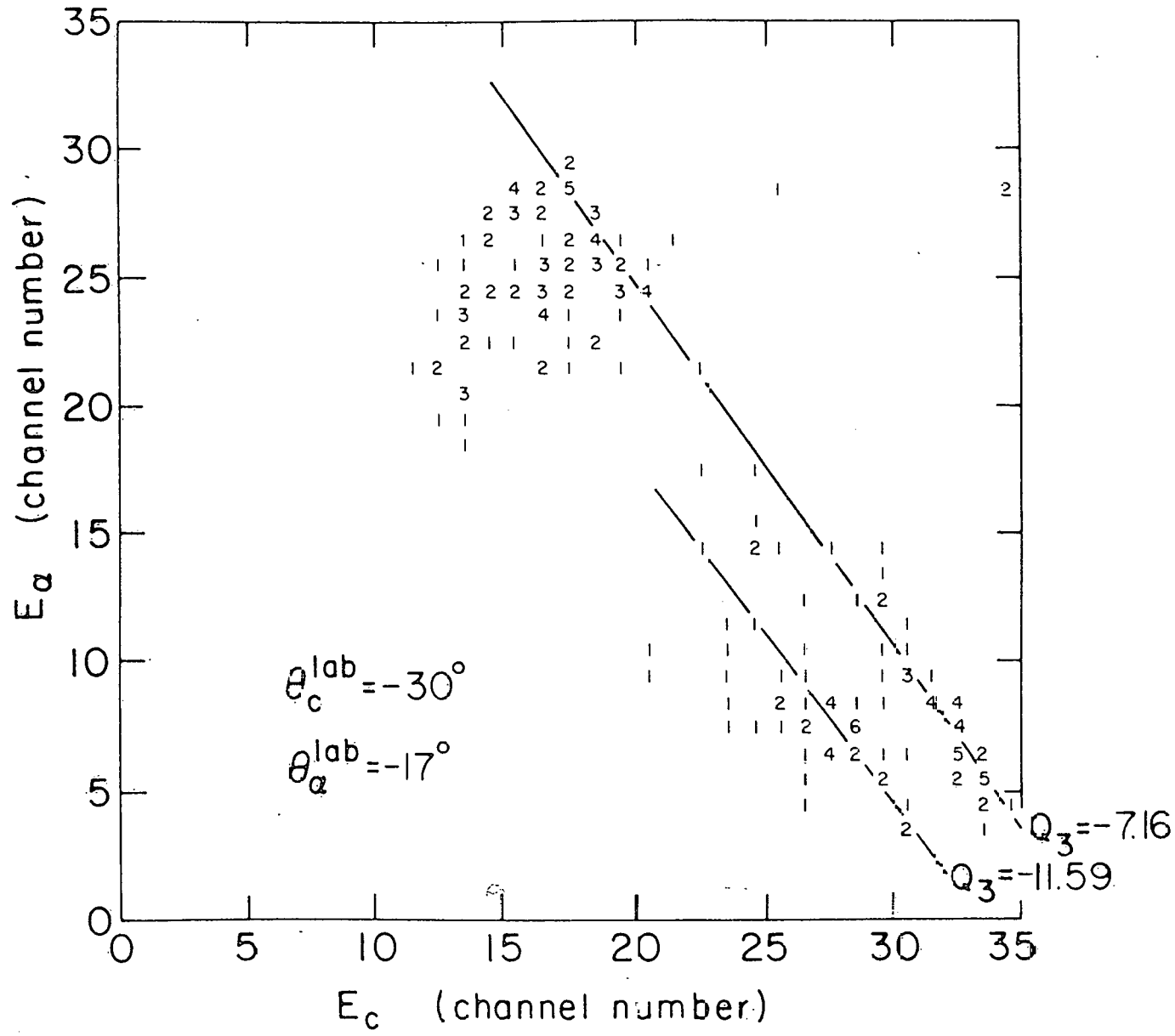
35
30
25
20
15
10
5
0
0
5
10
15
20
25
30
35
E_α (channel number)
E_c (channel number)
θ_c^{lab}=-30°
θ_α^{lab}=-17°
Q_3=-7.16
Q_3=-11.59

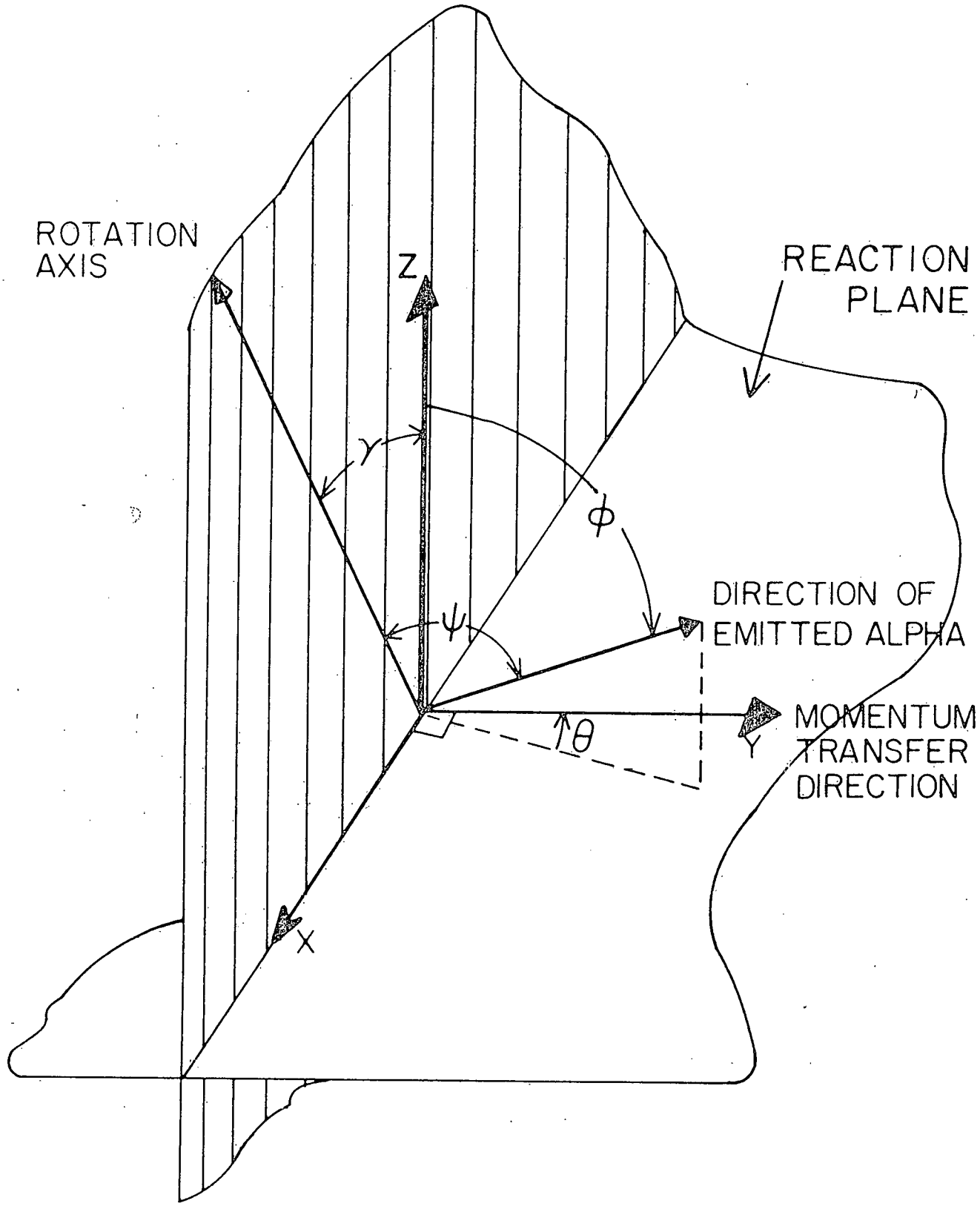
ROTATION
AXIS
Z
REACTION
PLANE
γ
φ
ψ
DIRECTION OF
EMITTED ALPHA
θ
Y
MOMENTUM
TRANSFER
DIRECTION
X

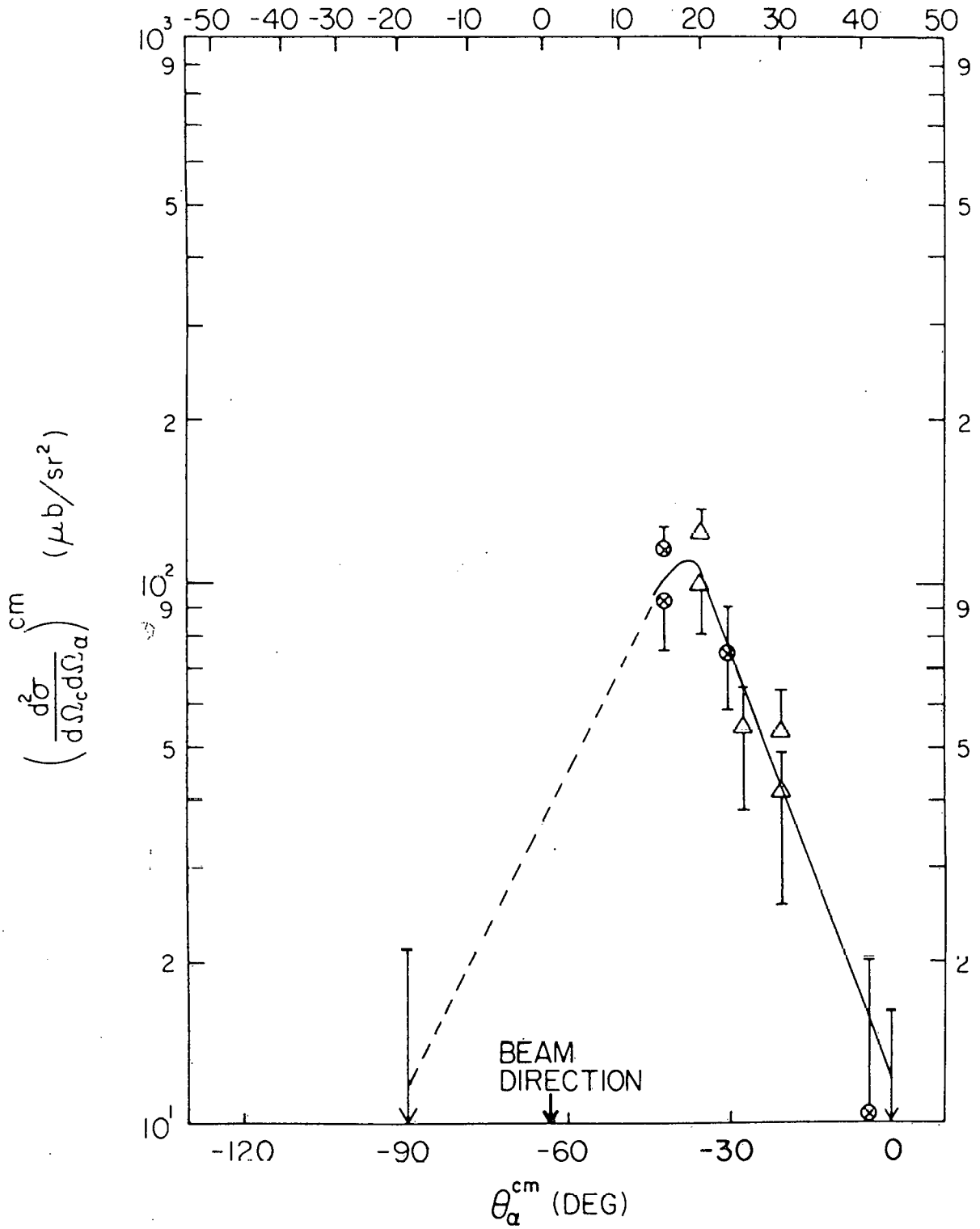
-50 -40 -30 -20 -10 0 10 20 30 40 50
10^3
9
5
2
10^2
9
5
2
10^1
$\left(\frac{d^2\sigma}{d\Omega_c d\Omega_\alpha}\right)^{cm}$ (μb/sr^2)
BEAM DIRECTION
-120 -90 -60 -30 0
θ_α^{cm} (DEG)

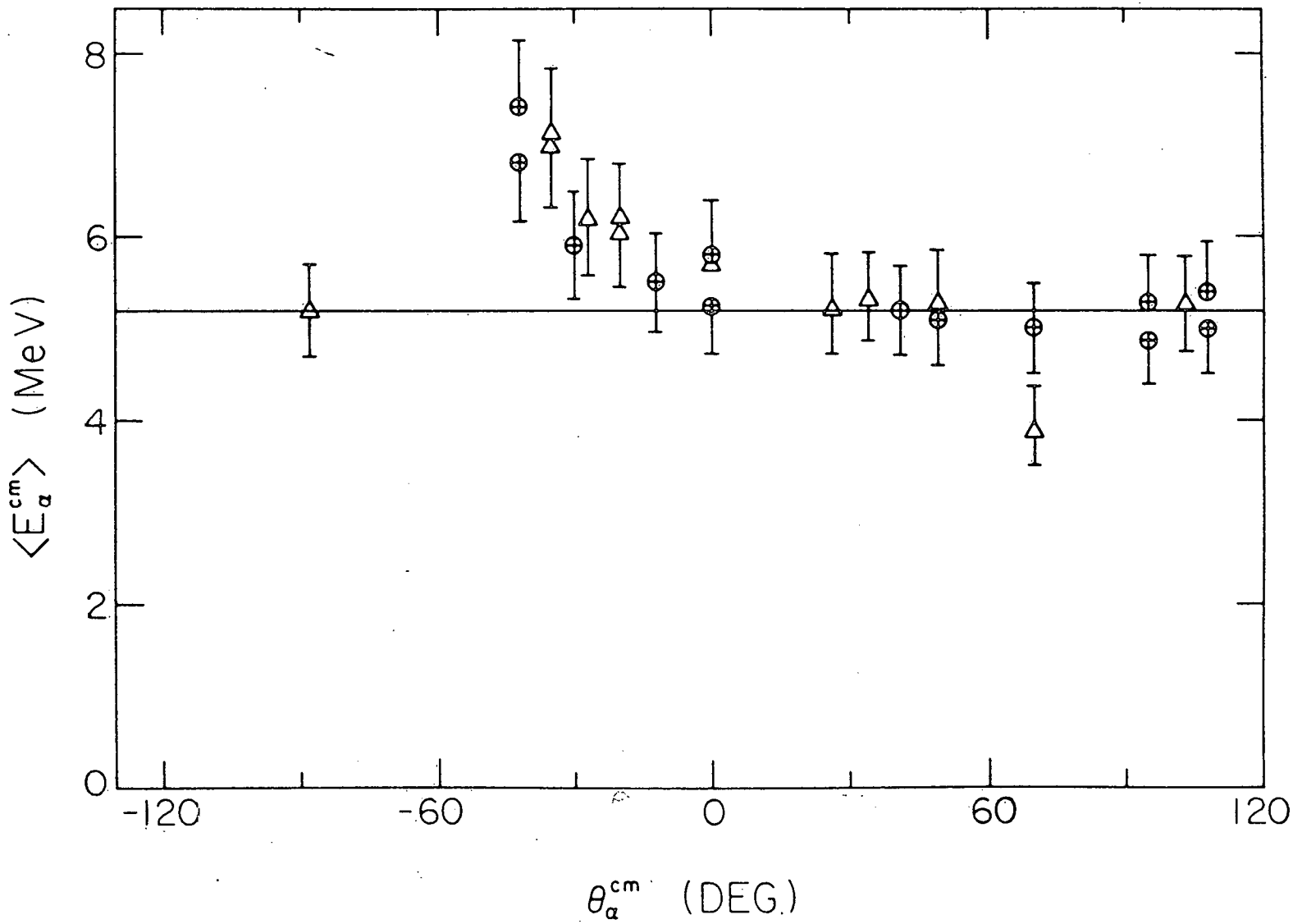
8
6
4
2
0
-120
-60
0
60
120
$\langle E_\alpha^{cm} \rangle$ (MeV)
θ_α^{cm} (DEG.)